RESEARCH PAPER

Incubation time fracture criterion for FEM simulations

Vladimir Bratov

Abstract The paper is discussing problems connected with embedment of the incubation time criterion for brittle fracture into finite element computational schemes. Incubation time fracture criterion is reviewed; practical questions of its numerical implementation are extensively discussed. Several examples of how the incubation time fracture criterion can be used as fracture condition in finite element computations are given. The examples include simulations of dynamic crack propagation and arrest, impact crater formation (i.e. fracture in initially intact media), spall fracture in plates, propagation of cracks in pipelines. Applicability of the approach to model initiation, development and arrest of dynamic fracture is claimed.

Keywords Fracture dynamics · Incubation time · Crack dynamics · Finite element method · Fracture arrest

1 Introduction

Numerical methods are of a vital importance while solving problems of dynamic fracture mechanics. First of all this is connected to the fact that an overwhelming majority of problems of dynamic fracture are impossible to solve analytically. Framework of dynamic problems allowing analytical solution is limited to few classical solutions (e.g. see the book of Freund [1]). Turning to problems of dynamic fracture evolution (fracture development and arrest) a possibility to construct an analytical solution is completely vanishing (not accounting for couple of available solutions for steady-state dynamic crack propagation).

V. Bratov (✉)
Institute for Problem in Mechanical Engineering
of the Russian Academy of Sciences,
Bolshoj pr. V.O. 61, 199178,
St.-Petersburg, Russia
e-mail: Vladimir@bratov.com

Central issue while solving problems of dynamic fracture (no matter, numerically or analytically) is a rupture criterion to be used in order to assess if fracture should occur at a given state of a system. For several decades, it is known that classical fracture criteria (criteria based on the idea of the ultimate stress for intact media and on the idea of the critical stress intensity factor for cracked bodies) are not able to provide satisfactory coincidence with known experiments (see e.g., Ref. [2]). Moreover, it is easy to show that these criteria contradict the common sense being applied to transient problems (as discussed in Ref. [3]).

In Refs. [2–4] a new criterion based on the introduced concept of the incubation time of a brittle fracture process was proposed in order to predict conditions of initiation of brittle fracture in solids undergoing dynamic impact loading. Later in this paper some aspects of the incubation time fracture criterion (ITFC) will be discussed in more detail. Exhaustive information about ideology and physics behind the ITFC and the incubation time can be found in a book by Morozov and Petrov [3]. In the same book one can find possible experimental schemes that can be used in order to evaluate the incubation time. Here some distinguishing properties of the ITFC that make it especially attractive to be embedded into numerical computational schemes are outlined.

In this connection, the important feature of the incubation time fracture criterion is that it is able to predict fracture initiation conditions with reliability and correctness in "static" case of "slow" changing loads and "slow" changing geometry as well as in "dynamic" case of high-rate loads and "fast" changing geometry (see e.g., Refs. [2, 4]. Moreover, the criterion is supplying a smooth transition between these two cases [5]. As a result, using this approach one does not need to care about time scale of the problem—the criterion is giving correct predictions in a wide range of loading rates from static problems to the extreme dynamic cases. Even distinguishing between "static" and "dynamic" situation is not obligatory needed anymore, though the ITFC itself is providing a perfect possibility to do this.

It is easy to show (see e.g., Ref. [6]) that for "static" problems with "slow" changing loads and "slow" changing geometry, the ITFC is coinciding with well-known Neuber–Novozhilov fracture criterion [7, 8]. It can be proven [3, 6, 9] that with the right choice of spatial parameter *d*, used in the criterion formulation, Neuber–Novozhilov criterion is giving predictions coinciding with critical tensile stress (ultimate stress) criterion in the case of rapture of initially intact media and the critical stress intensity factor (Griffith–Irwine, K_{IC}) criterion in the case of rupture in a tip of a macroscopic crack. The important outcome is that the criterion is governing two cases that are normally treated separately in a single (and rather simple) rupture condition—it can be applied to predict brittle fracture of materials with arbitrary size of defect, from intact undamaged media to media with macroscopic cracks. The Neuber–Novozhilov criterion is also providing smooth transition between these two cases. As a result the criterion is perfectly applicable to fracture problems with fracture surface geometry that is not known a priori. In such problems fracture in initially intact material can be initiated somewhere in a body and, as it evolves, transform into a macroscopic crack. The entire fracture evolution can be predicted with a single fracture criterion.

In a big number of works (see e.g., Refs. [3, 5, 10]), applying the introduced ITFC to predict critical fracture conditions in different dynamic fracture experiments (e.g., Ref. [11]) proved that the ITFC can be successfully used in order to predict initiation of brittle fracture appearing as a result of high-rate deformation applied somewhere in a body. In the same works, a material parameter τ — the incubation time of brittle fracture, constituting the essence of the ITFC and characterizing the temporal dependence of media strength was computed for many of widely used materials.

Lately an approach making it possible to embed the ITFC into numerical computational schemes based on finite element method (FEM) was developed [12–14]. Utilizing this approach simulation of several different experiments on dynamic impact fracture caused by high-rate loads was performed [12, 15]. These works testify that the ITFC used as a rupture criterion in FEM numerical simulations is able to predict correctly and precisely and all the variety of experimentally observed phenomena of dynamic fracture initiation, evolution and arrest.

As a matter of fact, not including the ITFC and approaches based on classical fracture criteria that are obviously inapplicable to predict high-rate fracture, nowadays only one approach exists is pretending to correct prediction of dynamic fracture. This approach is originating from the works of Freund [16–18] and was later developed by Rosakes. It is based on an assumption that fracture criterion in a tip of a crack can be received as a function of stress intensity factor rate: $K^d(t) \leq K_C^d(\dot{K}(t))$, with K^d being the dynamic stress intensity factor, changing in time, K_C^d being its critical value and dot denoting time derivative. As discussed by Bratov and Petrov [12], this approach in many cases is contradicting the common sense and is applicable to predict dynamic fracture initiation (not even mentioning high-rate fracture evolution) in a very limited set of problems with strict requirements on material, loading history, fractured sample geometry etc.

The main idea of this paper is to demonstrate that the ITFC is the most promising, precise and convenient among available criteria suitable for embedment into numerical codes in order to predict dynamic fracture. The paper is also giving information about the ITFC in connection with possibilities of its numerical implementation into FEM. The main problems of this implementation are discussed and the algorithm in order to embed the ITFC into FEM is explicitly given.

2 Numerical implementation of the incubation time fracture criterion

Incubation time criterion for brittle fracture at a Point *x* at time *t* reads as [2–4]

$$\frac{1}{\tau} \int_{t-\tau}^{t} \frac{1}{d} \int_{x-d}^{x} \sigma(x', t') \mathrm{d}x' \mathrm{d}t' \geq \sigma_c, \qquad (1)$$

where τ is the microstructural time of a brittle fracture process (or fracture incubation time)—a parameter characterizing the response of the studied material to applied dynamic loads (i.e. τ is constant for a given material and does not depend on problem geometry, the way a load is applied, the shape of a load pulse and its amplitude). *d* is the characteristic size of a fracture process zone and is constant for the given material and the chosen scale level. σ is a normal stress at a point, changing with time and σ_c is its critical value (ultimate stress or critical tensile stress found in quasistatic conditions). x' and t' are the local coordinate and time.

Assuming

$$d = \frac{2}{\pi} \frac{K_{IC}^2}{\sigma_c^2}, \qquad (2)$$

where K_{IC} is a critical stress intensity factor for Mode I loading (Mode I fracture toughness), measured in quasistatic experimental conditions. It can be shown that within the framework of linear elastic fracture mechanics for the case of fracture initiation in the tip of an existing crack, Eq. (1) is equivalent to

$$\frac{1}{\tau} \int_{t-\tau}^{t} K_I(t') \mathrm{d}t' \geq K_{IC}. \qquad (3)$$

Condition (2) arises from the requirement that Eq. (1) is equivalent to Irwin's criterion ($K_I \geq K_{IC}$), in the case of $t \to \infty$.

Once again it should be noticed that for slow loading rates and, hence, times to fracture that are much bigger than τ, Condition (3) for crack initiation gives the same predic-

tions as Irwin's criterion of a critical stress intensity factor. In the case when the stress field is not singular in the vicinity of Point x (locally intact material) and under condition of quasistatic load applied to the media, Condition (1) is reduced to critical tensile stress fracture criterion. It should be outlined that Eq. (1) in the quasistatic case is equivalent to critical stress intensity factor criterion under assumption that square root asymptotic solution is valid in the vicinity of a singular Point x. In the case of a singular field that is not controlled by a square root singularity (for example asymptotic field appearing in the tip of an angular notch), when Griffith-Irwin critical stress intensity factor criterion is not applicable, Condition (1) can be successfully used to predict fracture in such a singular point [19].

Thereby, Eq. (1) automatically ensures correct fracture prediction in a very wide range of quasistatic problems with materials fracturing following brittle scenario. It has been proven in multiple works (see e.g., Refs. [2–5, 10, 14]) that for dynamic problems equation (1) (under condition that incubation time τ is correctly identified for the studied material) is correctly predicting stressed state at the moment of initiation of brittle rupture (in the case of fracture of initially intact media, as well as in the case of initiation of macroscopic crack). First of all this concerns problems with loads applied at high and ultra-high rates.

In this work, it will be demonstrated that Condition (1) can be also used to predict evolution of quasi-brittle fracture (fracture and fragmentation of initially intact media, growth and arrest of macroscopic cracks etc.).

3 Numerical implementation

Several questions are to be discussed in connection to FEM implementation of the ITFC.

(1) FE mesh. Additional requirement to FE mesh to be used in simulation with the ITFC utilized as fracture criterion consists in limitation on the size of finite elements in a vicinity of points where rupture is possible. Obviously, the size of an element in this region should not exceed d (see Eq. (2)). Otherwise, it will not be possible to perform sufficiently precise spatial integration in fracture condition (1). Also, meshing the sample, one should keep in mind that material should be separated once fracture criterion is executed somewhere in the sample. This applies both to the choice of mesh in problems without adaptive meshing (mesh is not changing throughout the simulation) and the choice of adaptive mesh that can depend on current geometry of fracture zone and other factors.

(2) Time step. In order to have a possibility to perform sufficiently precise time integration in Eq. (1) one should require that the time integration step is small as comparing to incubation time τ of the material modeled.

(3) Control of fracture criterion (1) execution. Implementation of control of the fracture condition execution does strongly depend on a problem to be modeled. In some problems (for example, in the majority of problems on propagation of a macroscopic crack in unbounded media) fracture is possible only in a tip of an existing crack. In this case, it is sufficient to keep track of execution of the Condition (1) only in a single point (the tip of the crack). In other problems (for example, in the majority of problems on fracture of initially intact media) it is necessary to trace execution of Eq. (1) in rather extent zone or even in the whole modeled body. Under condition that the zone where implementation of Eq. (1) should be traced is defined and also that time step and mesh are correctly chosen, calculation of the left side in Eq. (1) does not make a big difficulty. In the examples presented later, in this paper execution of Eq. (1) is controlled by an external program after every computational time step. However, with the lapse of time it is planned to create special elements for commercial FEM packages (ABAQUS [20], ANSYS [21] etc.) with criterion (1) being explicitly embedded into their formulation. Creation of such elements will considerably simplify the problem and will give a possibility to completely automate numerical simulations of brittle fracture.

(4) Spatial size of fracture increment (2d problems). Incubation time theory for brittle fracture [4, 14] is introducing linear size corresponding to an elementary cell of fracture on a chosen scale level. This size can also be interpreted as a typical size for the defect that one can call fracture on the chosen scale level. This size d depends on modeled material and the scale level and can be computed using Eq. (2). It makes sense to consider that once Eq. (1) is implemented in some point of the modeled body, fracture surface should be increased by the size of the elementary fracture cell d. In this connection having zones where fracture is possible meshed by elements sized d seems to be a reasonable choice.

(5) Creation of a new surface. In finite element formulation there exist several possibilities to create a new surface appearing as a result of material fracture. In the case of a crack extending along symmetry axis (in problems with symmetry) node release technique can be utilized (see e.g., Ref. [12]). In problems without remeshing when fracture geometry is changed, node splitting technique or technique implying removal of restrictions on nodal dimensions of freedom (DOF's) [15] can be used. In other situations, one can use schemes assuming remeshing of the modeled body when fracture zone is changed (incremented). This approach is the most universal but at the same time the most difficult in implementation (apart from remeshing one should care about remapping of nodal values (displacements, velocities, accelerations) to new mesh). Remeshing and remapping also normally require substantial computational expense. The conclusion is that for every new problem technique to create a new surface should be specially chosen having in mind expense connected with model development and time needed for computations.

4 Examples

4.1 Dynamic crack propagation

To check the applicability of the criterion (1) to predict dynamic crack propagation, an attempt was made to simulate the classical fracture dynamics experiments reported by Ravi–Chandar and Knauss [11]. Detailed description of the model used in simulations and results of simulation of these experiments using FEM with the ITFC as a condition for crack extension can be found in Ref. [12]. Here, some basic principles and main results are presented.

In these experiments [11], a rectangular sample with a cut simulating a crack is loaded by applying an intense load pulse to the crack faces. Figure 1 presents the experimental scheme and Fig. 2 gives an approximation of the load applied to the crack faces. The sample behavior is described by equations of linear elasticity everywhere but the path of the crack, where fracture condition is given by Eq. (1). ANSYS [21] finite element package is used in order to solve linear elastic equations while implementation of Eq. (1) is controlled by an external program after every substep. The problem is symmetrical and the path of the crack is following the line of symmetry. This gives a possibility to model only half of the sample.
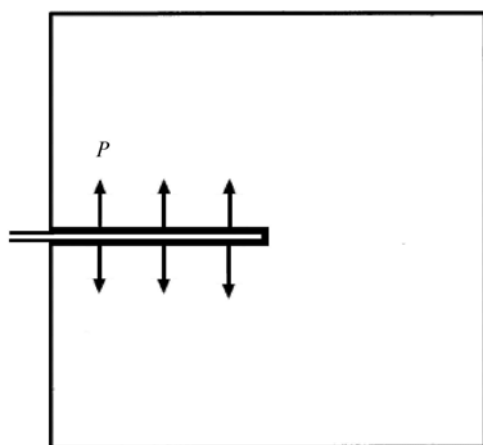
Fig. 1 Experimental scheme used by Ravi–Chandar and Knauss [11]

Nodes along the crack path are subjected to symmetrical boundary conditions up to the moment when the condition (1) is satisfied at a particular node (node movements in the vertical direction are restricted). At this moment the restriction on movement of the particular node is removed and a new surface is created. The technique used is similar to the node release technique.
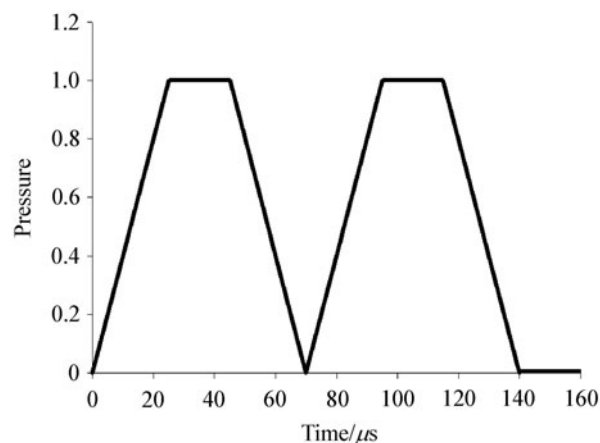
Fig. 2 Temporal shape of pressure pulse released in experiments by Ravi–Chandar and Knauss [11]

Rectangular 4-node elements were used to mesh a body. The size of elements along the crack path was taken to be exactly d (see Eq. (2)). A total of 18 621 nodes and 18 404 elements were used to form the mesh. Small elements with sizes equal to d are placed adjacent to the crack path to provide the needed accuracy of computation. Distant elements are larger in order to minimize the computational time and expense.

The shape of the pressure pulse applied to the crack faces is given by Fig. 2, and its amplitude A is alternated in simulations. Material parameters typical for Homalite-100, used in the experiments of Ravi–Chandar and Knauss, were used in the calculations. These parameters are presented in Table 1. The microstructural time of the fracture process, τ, for Homalite-100 was found in Ref. [5] from the analysis of experiments presented in Ref. [11]. The values of the critical stress intensity factor and the ultimate tensile stress gives a value for d. It appears to be 0.1 mm for Homalite-100 on a laboratory size scale.

Table 1 Properties of Homalite-100 used in numerical simulations

Density $\rho/(\text{kg·m}^{-3})$	1 230
Young's modulus E/MPa	3 900
Poisson's ratio ν	0.35
Critical stress intensity factor $K_{\text{IC}}/(\text{MPa}\sqrt{\text{m}})$	0.48
Ultimate tensile stress $\sigma_{\text{c}}/\text{MPa}$	48
Incubation time of fracture $\tau/\mu\text{s}$	9

Unfortunately in the paper by Ravi–Chandar and Knauss, there was no information about amplitude of the load given graphically in Fig. 2. Performing multiple ANSYS computations for different amplitudes it was found that amplitudes around 5 MPa result in crack extension histories very close to those observed by Ravi–Chandar and Knauss [11]. In Fig. 3 the computational result for A =

5.1 MPa is compared to the experiments reported by Ravi–Chandar and Knauss.
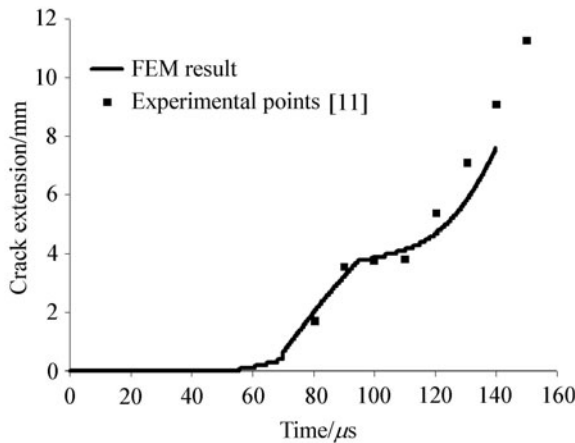
Fig. 3 Crack extension history. Comparison of simulation results to experimental points received in Ref. [11]

It is demonstrated that utilizing the FE code solving the problem of linear elasticity joint with the ITFC (1) used to predict critical condition for crack extension, it is possible to correctly predict evolution of dynamically loaded cracks. Apparently the ITFC with d chosen from the condition that Eq. (1) coincides with Griffith-Irwine fracture criterion in quasistatic conditions, can be utilized in order to predict initiation, growth and arrest of dynamic cracks. This approach can be also used to predict growth of cracks with paths that are not known a priori (i.e. cracks that can change growth direction and branch). In this case one should check for Eq. (1) implementation on all the planes passing through the crack tip (all the possible orientations).

4.2 Impact crater formation (fracture of initially intact media)

In this section, an attempt to incorporate incubation time approach into finite element (FE) code and to simulate conditions of satellite SMART1 lunar impact conducted by ESA year 2006 [22, 23] is presented. Aim of the simulation is to compare dimensions of crater created due to SMART1 contact to the moon surface to results received using FE method utilizing the ITFC as the critical rupture condition.

The traditional way to create new surface in FE formulation is associated with splitting of existing nodes. Using this approach is reasonable in most cases, though this normally requires remeshing and remapping, that are rather time consuming procedures. For the studied problem the situation is different. To guarantee correct integration in Eq. (1) one should use small (as comparing to τ) time steps. Thus the solution is resulting in long series of tiny substeps. Solution (convergence) on every substep is achieved comparably fast—FE solver is almost not iterating. It was found that in this case it is more effective to use multiple nodes in the

same location from the beginning, rather than split the node in question. Each element the full model is constructed of, is not sharing nodes with other elements.

2-D problem with rotational symmetry is solved. Quadratic 4-node elements are used. Dimensions of every element is exactly d times d (where d is given by Eq. (2)). Obviously, 4 nodes have the same location for inner points of a body and 2 nodes have the same location for the points belonging to the boundary. These nodes originally have their DOF's coupled. This results in exactly the same FE solution before the fracture condition is implemented in a respective point as if elements had shared nodes. When the fracture condition is fulfilled, restriction on nodes DOF's is removed—a new surface is created. This is done automatically by FE code after every substep.

Figure 4 gives a schematic representation of internal points of a body. Originally all 4 nodes sharing the same location have all of their DOF's coupled. Condition (1) for this point can be written as

$$\frac{1}{\tau} \int_{t-\tau}^{t} \sigma_{ii}(t^*) \mathrm{d}t^* \sigma_\mathrm{c}, \qquad i = 1, 2. \tag{4}$$

Repeating indices do not dictate summation in this case. Spatial integration is removed, because the stress in the respective direction calculated by FE program is already a mean value over size d (since d is the element size being used). If Eq. (4) is fulfilled for σ_{11} and σ_{22} then displacements of nodes 1, 2, 3 and 4 on Fig. 4 get uncoupled. If Eq. (4) is fulfilled for σ_{11}, two new couple sets consisting of nodes 1, 2 and 3, 4 are created. If Eq. (4) is fulfilled for σ_{22}, new couple sets are created for nodes 1, 3 and 2, 4. For later times condition (4) in applicable direction is traced for newly created couple sets separately. Contact between separated fragments is not modeled.
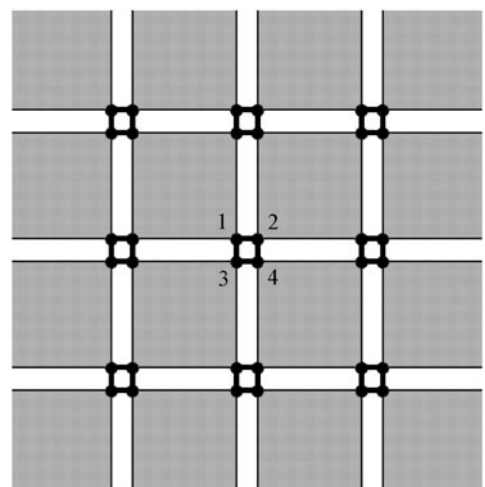
Fig. 4 Model consisting of elements without shared nodes

The problem is solved for half-space. Half-space representing the moon had following material properties: $\sigma_\mathrm{c} =$

10.5 MPa, $K_{IC} = 2.94$ MPa $\sqrt{m}$, $\tau = 80\,\mu s$, $E = 60$ GPa, $\rho = 2\,850$ kg/m^3, $\nu = 0.25$ typical for earth basalt. This results in $d = 5$ cm. Half-space is impacted by a cylinder with diameter of 1 m and height of 1 m. Density for the cylinder is chosen so that its mass is the same as the one of SMART1 satellite. We suppose material of cylinder is linear elastic and has no possibility to fracture. Elastic properties are: $E = 200$ GPa, $\nu = 0.32$, typical for steel. SMART1 satellite had a form close to cubic with side of 1 m and had a mass of 366 kg. SMART1 impacted the moon surface at a speed of approximately 2 000 m/s. In FE formulation the cylinder was given an initial speed of 2 000 m/s prior its contact to the half-space boundary. Figure 5 gives an overview of the FE model. Size of the sample, representing the half-space is chosen from the condition that the waves reflected from the sample boundaries are not returning to the region where the crater is formed in the process of the simulation. The total of 17 328 nodes and 17 252 elements were used in FE model. Time step was chosen to be equal to time needed for the fastest wave to pass the distance equal to d.
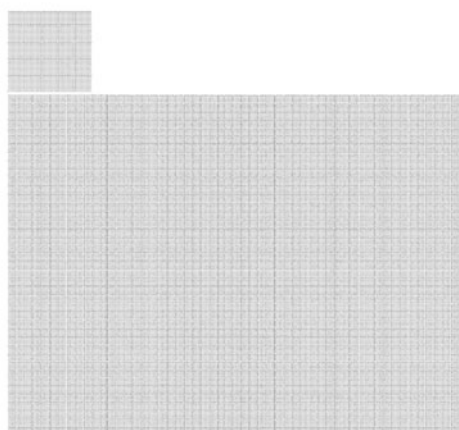

Fig. 5 FE model overview

ANSYS finite element package [21] was used to solve the stated problem. Control of the fracture condition (4) fulfillment in all of the sample points and new surface creation when rupture criterion is implemented was carried out by a separate ANSYS ADPL subroutine.

Figure 6 shows the sample state after the simulation is finished. Damage localized at down part of the sample is due to finite dimensions of a sample and represent cleavage fracture that occurred after compressive waves have reflected from lower boundary. In Fig. 7, locations of nodes where the fracture occurred are marked. This gives a possibility to assess dimensions of crater that is formed after the SMART1 impact. Damaged zone is found to be about 10 m in diameter and about 3 m deep. Zone where the material is fully fragmented (crater formed) can be assessed having 7–10 m in diameter and 3 m deep. This result is coinciding with ESA estimations of dimensions of crater formed due to SMART1 impact [22, 23].
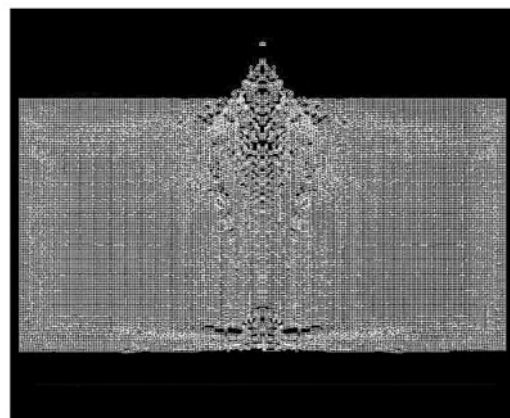

Fig. 6 The sample after impact
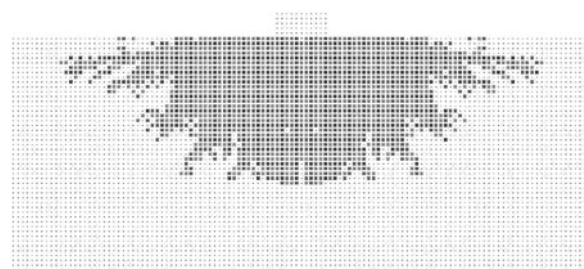
Fig. 7 Locations of ruptured nodes

4.3 Spall fracture in plates

Utilizing method used while modeling SMART1 lunar impact it is possible to perform simulations in rather extent class of problems including brittle fracture of different materials. In this example spall fracture in a circular plate was studied. One of the plate's surfaces is loaded by dynamic pressure pulse having rectangular time-shape. Duration of the load is supposed to be small as comparing to the time needed for the fastest wave to travel the distance equal to the plate's thickness. Compressive stresses are changing their sign being reflected from the free surface of the plate and tension stresses are appearing at some distance from the free surface of the plate (for loads with rectangular time-shape this distance is equal to half-distance the longitudinal wave can travel within load duration). For pressure pulses with sufficient amplitude fracture takes place as a result of emerging tensile stresses. This scheme is typical for many, if not the majority of dynamic fracture experiments. In Fig. 8, results of one of the experiments modeled are presented graphically. As one can see from the presented figures, fracture received in numerical computation is qualitatively repeating fracture observed in experiments on spall fracture in impacted plates.
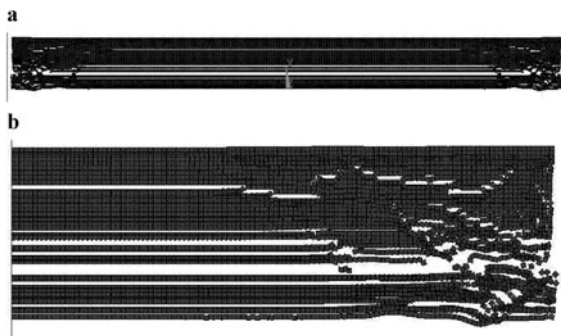
Fig. 8 a View of a plate with spall fracture; **b** View of a plate with spall fracture (magnification)

4.4 Growth of crack in gas pipeline

In the last of the presented examples, the developed approach is applied to simulate growth of a dynamic crack in a gas pipeline. Finite element model giving a possibility to predict fracture of gas pipeline subjected to quasistatic and dynamic loads is developed. It is assumed that the crack can grow along the line parallel to the pipe axis. Used finite element mesh is presented in Fig. 9. Computations were performed for 1/4 of the presented model (symmetry across planes *ZX* and *XY* is used).
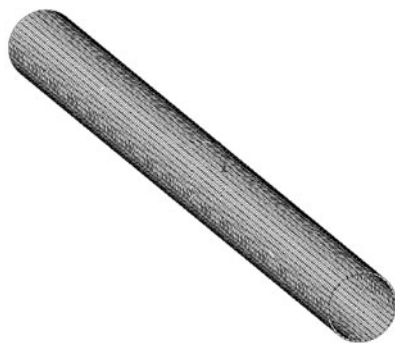


Fig. 9 FE model of gas pipeline

Simulation is performed for pipeline with length of 18 m. Pipeline diameter is 1.22 m. 36 600 nodes and 17 940 elements are used in the FE model.

The pipeline is loaded by internal pressure close to operational pressures in gas pipelines. Drop of pressure in the pipeline as a result of crack extension was modeled as movement of two wavefronts: the front of the front wave of pressure drop (velocity of this front is equal to velocity of the acoustic wave in gas—about 400 m/s for natural gas) and the back front of pressure drop travelling at a lower speed. After passage of the back front the pressure inside the pipeline is equal to the external atmospheric pressure. Between the two fronts pressure is supposed to be linearly dependent on coordinate (Fig. 10).
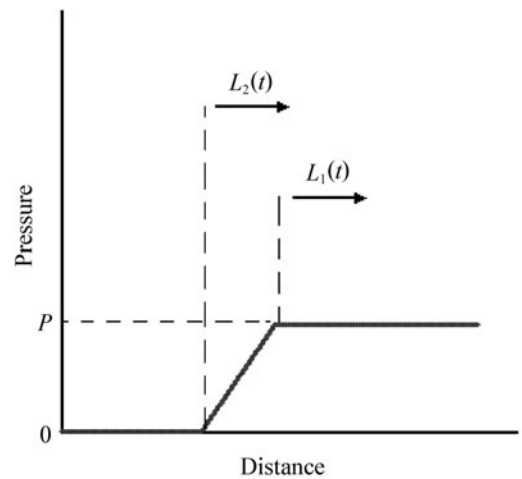

Fig. 10 Model for pressure drop

The pipeline was quasistatically loaded by internal pressure. Fracture was initiated by a small defect (crack) that was artificially introduced. This is imitating appearance of a crack in a pipeline (for example, fatigue crack). When the defect is introduced it starts to grow if the internal pressure is big enough to advance defect of the introduced size. In Fig. 11 view of the pipeline is presented for different times.
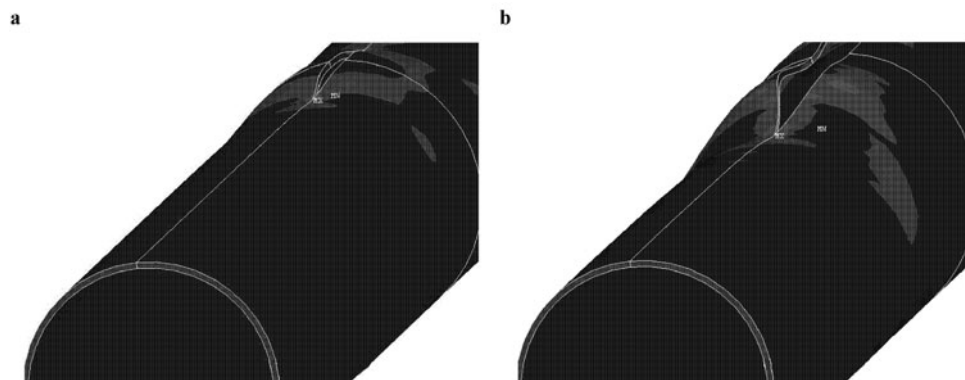
Fig. 11 Pipeline with a macroscopic crack. Diameter of the pipe is **a** 1.22 m; **b** 1.22 m; **c** 1.22 m
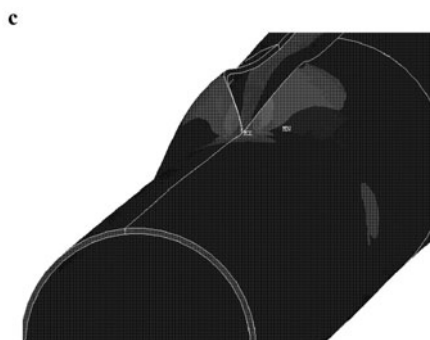
Fig. 11 Pipeline with a macroscopic crack. Diameter of the pipe is **a** 1.22 m; **b** 1.22 m; **c** 1.22 m (Continued)

It was found that in the modeled situation the speed of the crack is close to the speed of the acoustic wave in gas that determines the speed of the front of the pressure drop. This leads to a conclusion about instability of crack propagation regimes in the modeled situation—a small change in properties of the pipeline material can result in qualitative change it crack propagation regime: should the speed of the crack be higher than the speed of acoustic signal in gas, the crack will never arrest.

Received instability of crack propagation regimes is in a good coincidence with experiments on dynamic cracking in gas pipelines. In these experiments, a section of gas pipe was loaded by internal pressure close to operational pressure inside the gas pipeline. A furrow was made in the part of the pipe parallel to its central axis. The furrow was filled with an explosive substance. When the explosive is blasted the crack starts to propagate from the furrow. Pipelines made of several different pipe steels were tested. It was found that length of the resulting crack does strongly depend on material of the pipeline and the length of the resulting crack does vary significantly (from 3 m to 300 m) though all steels had very similar properties. The origin of this instability was understood due to numerical analysis presented above.

5 Conclusions

It was demonstrated that the area where the incubation time criterion for brittle fracture can be successfully used in order to simulate fracture is rather extent. An overwhelming majority of practical problems in dynamic fracture can not be solved analytically and require numerical methods to be used in order to receive the solution. In this connection the incubation time approach had significant advantages—it is applicable to predict both in static and dynamic fracture. Thus, there is no necessity in having different fracture criteria for different load rates. It was demonstrated that the ITFC embedded into finite element code is giving a possibility to predict initiation, development and arrest of dynamic fracture.

All this gives a reason to recommend the ITFC to be included into commercial and research FE codes as standard fracture criterion to be utilized while modeling structures that can undergo loads of the dynamic range.

References

1 Freund, L.B.: Dynamic Fracture Mechanics. Cambridge University Press, Cambridge (1990)

2 Petrov, Y.V., Morozov, N.F.: On the modeling of fracture of brittle solids. J. Appl. Mech. **61**, 710–712 (1994)

3 Morozov, N., Petrov, Y.: Dynamics of Fracture, Springer-Verlag, Berlin (2000)

4 Petrov, Y.V.: On "quantum" nature of dynamic fracture of brittle solids. Dokl Akad Nauk USSR, **321**, 66–68 (1991)

5 Petrov, Y.V., Morozov, N.F., Smirnov, V.I.: Structural micromechanics approach in dynamics of fracture. Fatig. Fract. Eng. Mater. Struct. **26**, 363–372 (2003)

6 Bratov, V.: Energy behavior in dynamic fracture of materials. Dissertation, St. Petersburg State University (2004)

7 Neuber, H.: Kerbspannunglehre: Grundlagen fur Genaue Spannungsrechnung, Springer-Verlag, Berlin (1937)

8 Novozhilov, V.V.: About the necessary and sufficient brittle strength criterion. Prikl. Mat. Mekh. **33**(2), 212–222 (1969)

9 Kornev, V.M., Kurguzov, V.D.: Interrelation between toughness and both strength and structural parameters of material. Int. J. Fract. **128**, 195–203 (2004)

10 Petrov, Y.V., Sitnikova, E.V.: Dynamic cracking resistance of structural materials predicted from impact fracture of an aircraft alloy. Tech. Phys. **49**(1), 57–60 (2007)

11 Ravi–Chandar, K., Knauss, W.G.: An experimental investigation into dynamic fracture: I. Crack initiation and arrest. Int. J. Fract. **25**, 247–262 (1984)

12 Bratov, V., Petrov, Y.: Application of incubation time approach to simulate dynamic crack propagation. Int. J. Fract. **146**, 53–60 (2007)

13 Bratov, V., Petrov, Y.: Optimizing energy input for fracture by analysis of the energy required to initiate dynamic mode I crack

growth. Int. J. Solid Struct. **44**, 2371–2380 (2007)

14 Bratov, V., Morozov, N., Petrov, Y.: Dynamic Strength of Continuum. St. Petersburg University Press, St. Petersburg (2009)

15 Bratov, V.A., Morozov, N.F., Petrov, Y.V.: Simulation of smart1 satellite impacting the moon surface. Dokl. Phys. **419**(1), 54–58 (2008)

16 Freund, L.B.: Crack propagation in an elastic solid subjected to general loading. I: Constant rate of extension. J. Mech. Phys. Solid **20**, 129–140 (1972)

17 Freund, L.B.: Crack propagation in an elastic solid subjected to general loading. II: Nonuniform rate of extension. J. Mech. Phys. Solid **20**, 141–152 (1972)

18 Freund, L.B.: Energy flux into the tip of an extending crack in an elastic solid. J. Elast. **2**, 341–349 (1972)

19 Kashtanov, A., Petrov, Y.: Fractal models in fracture mechanics. Int. J. Fract. **128**, 271–276 (2004)

20 ABAQUS: ABAQUS/Standard User's Manual, HKS Inc., USA (2002)

21 ANSYS: User's Guide, Release 11.0. ANSYS Inc., Pennsylvania, USA (2006)

22 ESA: Impact landing ends SMART-1 mission to the Moon. Available online. http://www.esa.int/esaCP/SEM7A76LARE_index_0.html Accessed 20 May 2011 (2006)

23 ESA, 2006b. Intense final hours for SMART-1, Available online. http://www.esa.int/esaCP/SEMV386LARE_index_0.html Accessed 20 May 2011 (2006)